

## Molecular Docking Reveals a Novel Binding Site Model for Fentanyl at the $\mu$ -Opioid Receptor

Govindan Subramanian, M. Germana Paterlini, Philip S. Portoghesi, and David M. Ferguson\*

Department of Medicinal Chemistry and Minnesota Supercomputer Institute, University of Minnesota, Minneapolis, Minnesota 55455

Received July 19, 1999

The ligand binding modes of a series of fentanyl derivatives are examined using a combination of conformational analysis and molecular docking to the  $\mu$ -opioid receptor. Condensed-phase molecular dynamics simulations are applied to evaluate potential relationships between ligand conformation and fentanyl substitution and to generate probable "bioactive" structures for the ligand series. Automated docking of the largely populated solution conformers identified a common binding site orientation that places the *N*-phenethyl group of fentanyl deep in a crevice between transmembrane (TM) helices II and III while the *N*-phenylpropanamide group projected toward a pocket formed by TM-III, -VI, and -VII domains. An analysis of the binding modes indicates the most potent fentanyl derivatives adopt an extended conformation both in solution and in the bound state, suggesting binding affinity may depend on the conformational preferences of the ligands. The results are consistent with ligand binding data derived from chimeric and mutant receptor studies as well as structure–activity relationship data reported on a wide range of fentanyl analogues. The binding site model is also compared to that of *N*-phenethylnormorphine. An overlay of the bound conformation of the opiate and *cis*-3-methylfentanyl shows the *N*-phenethyl groups occupy equivalent binding domains in the receptor. While the cationic amines of both ligand classes were found docked to an established anchor site (D149 in TM-III), no overlap was observed between the *N*-phenylpropanamide group and the remaining components of the opiate scaffold. The unique binding mode(s) proposed for the fentanyl series may, in part, explain the difficulties encountered in defining models of recognition at the  $\mu$ -receptor and suggest opioid receptors may display multiple binding epitopes. Furthermore, the results provide new insight to the design of experiments aimed at understanding the structural basis to the differential selectivities of ligands at the  $\mu$ -,  $\delta$ -, and  $\kappa$ -opioid receptors.

### Introduction

Ever since the discovery of fentanyl (**1**) in 1962 by Janssen,<sup>1</sup> the 4-anilidopiperidines have been exploited for developing highly selective  $\mu$ -opioid agonists<sup>2</sup> with specific pharmacological properties.<sup>3</sup> Over the last four decades, structure–activity relationship (SAR) studies of fentanyl analogues have provided considerable insight into the key structural features and pharmacophore elements required for high-affinity binding to the  $\mu$ -receptor.<sup>2,4</sup> In comparing fentanyl with the classic  $\mu$ -opiate morphine, certain similarities are apparent. Both compounds possess a protonatable nitrogen and an aromatic group that are commonly thought to mimic the *N*-terminal tyrosine moiety of opioid peptides.<sup>5</sup> However, SAR studies of *N*-phenolic derivatives<sup>6</sup> of fentanyl have shown that hydroxy substitutions do not influence the morphinomimetic potency of these compounds. Conversely, a dramatic loss in ligand binding is observed when the *N*-phenethyl group of **1** is replaced with the *N*-methyl group of morphine.<sup>7</sup> This suggests that fentanyls and  $\mu$ -opiates may display unique recognition elements to the  $\mu$ -receptor but induce qualitatively similar pharmacological profiles through different mech-

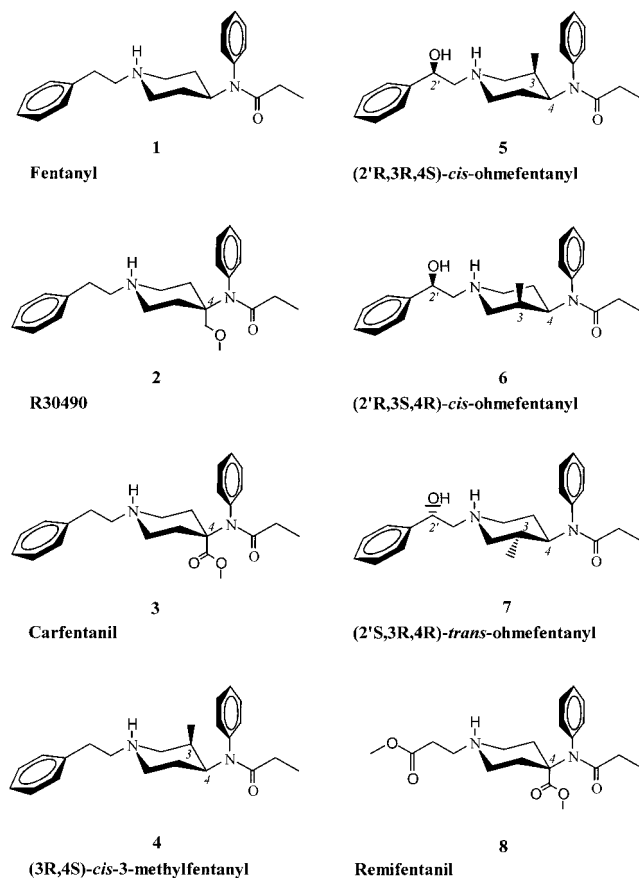
anisms that cannot be rationalized by structural comparisons alone.

Some hints to the recognition elements that may confer high-affinity binding to the  $\mu$ -receptor can be found in the SAR data reported on fentanyl. Substitutions to the piperidine ring have been shown to dramatically affect ligand binding (Table 1).<sup>8</sup> A simple methoxymethyl (as in R30490, **2**)<sup>9</sup> or acetate (as in carfentanil, **3**)<sup>10</sup> substituent on the piperidine 4-axial position of **1** has been shown to increase the ligand binding affinity by 45- and 160-fold, respectively. As alluded to above, substitution of the *N*-phenethyl group effectively abolishes ligand binding in some cases.<sup>7</sup> SAR studies have further revealed that compounds which retain the ethyl spacer display high affinity to the  $\mu$ -receptor. Fentanyls have also shown to display great variation in enantiospecific binding. With two chiral centers and four possible enantiomers, the most active *cis*-3*R*,4*S* stereoisomer of 3-methylfentanyl (**4**)<sup>11,12</sup> exhibits 7000-fold increased in vivo potency compared to morphine.<sup>13</sup> Perhaps, the most significant results have come from studies of 2'-OH-3-methylfentanyl (Figure 1). Out of the eight optically active isomers, *cis*-(2'*R*,3*R*,4*S*)-ohmefentanyl (**5**) belongs to the "super potent" class of  $\mu$ -selective agonists.<sup>14</sup> In contrast, the corresponding antipode *cis*-(2'*R*,3*S*,4*R*)-ohmefentanyl (**6**) is the least potent, weakly bound ligand in the ohmefentanyl series.

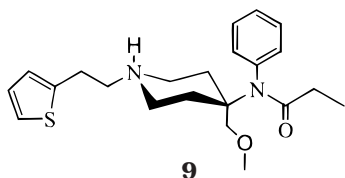
\* To whom correspondence should be addressed. Tel: 612-626-2601. Fax: 612-626-4429. E-mail: ferguson@vwl.medc.umn.edu.

**Table 1.** Experimental Binding Affinity (nM) of **1–7** for the  $\mu$ -,  $\delta$ -, and  $\kappa$ -Opioid Receptor

ligand	$K_i(\mu)$	$K_i(\delta)$	$K_i(\kappa)$	ref
<b>1</b>	3.97	1035	196.5	12b
<b>2</b>	0.089	23	63	26b
<b>3</b>	0.024	3.28	43.1	26b
<b>4</b>	0.02	77.3	57.4	42
<b>5</b>	0.013	103.4	122.2	42
<b>6</b>	47.7	>1.5 $\mu$ M	>0.5 $\mu$ M	42
<b>7</b>	0.06	200		14e

**Figure 1.** Structures of fentanyl derivatives **1–8**.

Among the four *trans* stereoisomers, the  $2'S,3R,4R$  enantiomer **7** possesses an enhanced affinity for the  $\mu$ -receptor as compared to the  $2'R,3R,4R$  counterpart. Of the various *N*-phenethyl modifications that have been reported,<sup>15</sup> remifentanyl (**8**) is one of the most unique.<sup>16,17</sup> This highly selective compound contains a hydrolytically labile ester group in place of the phenyl ring and, while sterically smaller than **1–7**, displays similar potencies.



Although SAR data provide insights into the pharmacophore features imparting specificity for the  $\mu$ -receptor binding, attempts to understand the structural basis for ligand recognition have been hindered by the difficulties in obtaining the crystal structure of the receptor or the ligand-bound complex. Fortunately, some

insights on the ligand binding domain have been gained through binding studies of fentanyl and related compounds using cloned opioid receptors. Chimeric constructs of opioid receptors have shown transmembrane (TM) helices I–III, VI, and VII to be involved in sufentanil (**9**) binding.<sup>18</sup> More specifically, site-directed mutagenesis data suggest that an aspartate residue in TM-III may be a critical anchor point for the binding of fentanyl derivatives.<sup>19</sup> This aspartate is highly conserved in opioid and related G-protein-coupled receptors and is thought to form a salt bridge with the protonated amino group of a variety of ligands. Although the binding data is limited, available pharmacological results<sup>20a,21</sup> strongly suggest fentanyls bind in the TM domain of the  $\mu$ -opioid receptor.

Despite the importance of fentanyl and related compounds in pain management, a detailed investigation of the receptor–ligand interactions responsible for high-affinity binding and selectivity to the  $\mu$ -receptor has not yet been reported. This is partly due to the inherent difficulties in modeling opioid receptors at a molecular level and also to the manifold conformations fentanyl may adopt in the condensed phase. Mosberg et al.<sup>22</sup> recently proposed a docking arrangement for *cis*-methylfentanyl to the  $\mu$ -opioid receptor. However, the focus of that study was on receptor model building, so the ligand docking results are quite limited. The “manual docking” performed places the ligand (**4**) toward the top of the receptor cavity and consequently does not completely explain available site-directed mutagenesis and chimeric data.<sup>18–21</sup> In addition, the conformational variability of **4** was not fully considered, potentially biasing the results. Although a number of computational studies on the conformational preferences of fentanyl analogues have been reported,<sup>23–27</sup> no conclusive agreement has emerged with respect to the *bioactive conformer* for members of this ligand series.

In this study, we combine SAR and ligand binding data with molecular docking experiments to understand the molecular determinants governing the recognition of fentanyls at the  $\mu$ -receptor. Using molecular dynamics (MD) simulations in the condensed phase, the most populated conformations of **1–8** are identified and docked to the human  $\mu$ -receptor (Figure 2). A refined  $\mu$ -opioid receptor model is also reported that takes advantage of the 6 Å projection map of bovine rhodopsin<sup>28</sup> and other biophysical data obtained from rhodopsin-like receptors. As in our earlier work on arylacetamides,<sup>29b</sup> an automated docking protocol is applied to evaluate the binding site orientations in this receptor model. The results are compared with available site-directed mutagenesis, chimeric, and SAR data to identify key ligand–receptor interactions involved in the molecular recognition process. Finally, the results are applied to provide new insight to the design of experiments aimed at understanding the structural basis to the differential selectivities of ligands at the  $\mu$ -,  $\delta$ -, and  $\kappa$ -opioid receptors.

## Computational Methods

**$\mu$ -Receptor Model.** The structural model of the human  $\mu$ -opioid receptor has been derived from electron cryomicroscopy data<sup>30</sup> and the  $C_\alpha$  coordinate template provided by Baldwin.<sup>28</sup> That template was generated from rhodopsin projection data in combination with a sequence analysis of 493

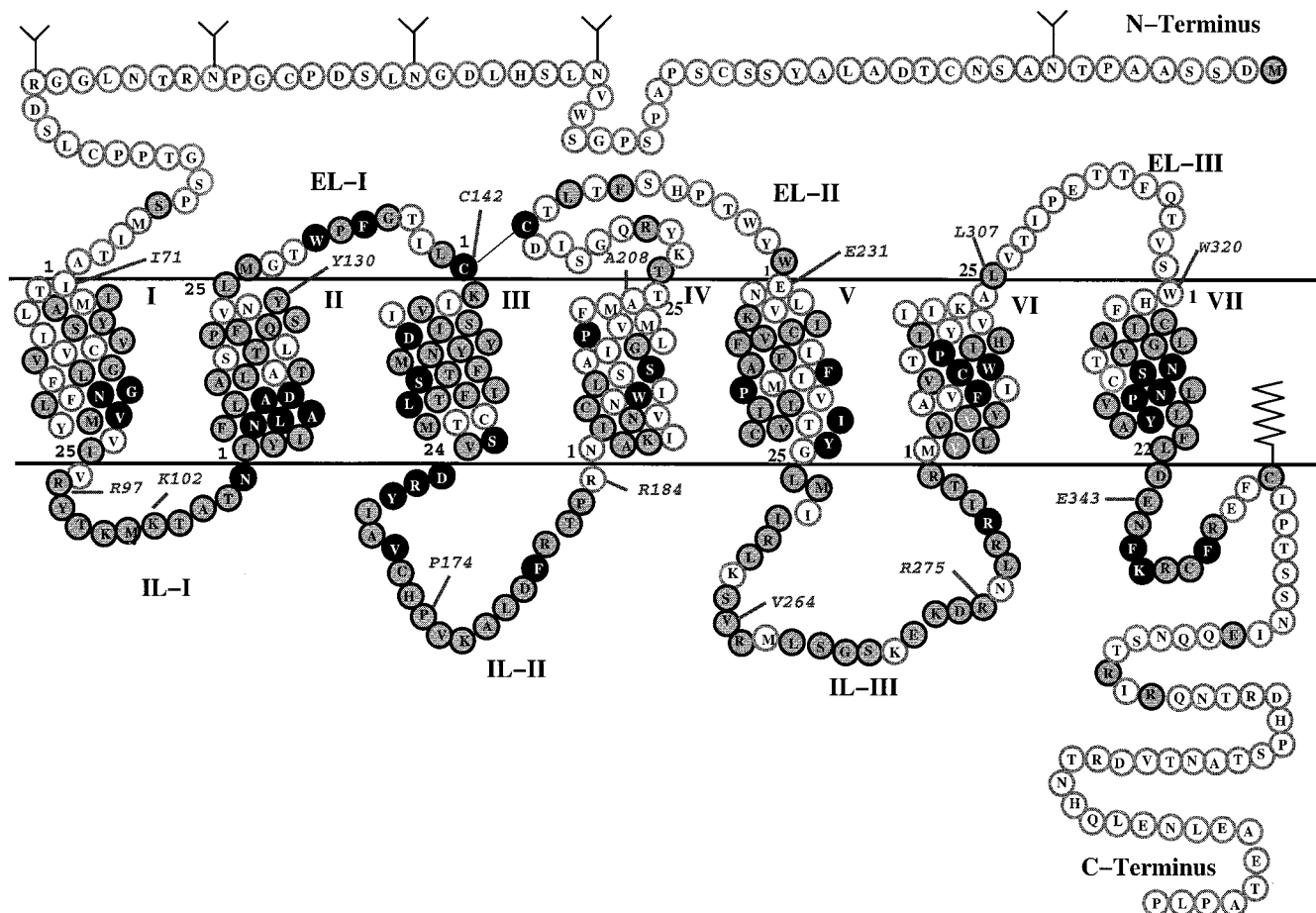


**Figure 2.** Serpentine model of human  $\mu$ -opioid receptor sequence. Solid black lines represent the approximate membrane boundaries. Filled black circles indicate the conserved residues in the aminergic receptor superfamily. Filled gray circles illustrate the residues conserved among the  $\mu$ -,  $\delta$ -, and  $\kappa$ -opioid receptors. The TM helices are denoted by roman numerals. The arabic numbers indicate the position of the residues inside the TM domain. The residue numbers in italics pertain to the overall sequence numbering and also indicate the starting and ending residue used in the present receptor model. Glycosylation sites in the N-terminus and palmitoylation site in the C-terminus are also shown. IL = intracellular loop and EL = extracellular loop.

GPCRs, including opioid receptors.<sup>28</sup> Substitution of the opioid receptor sequence (SWISS-PROT accession number, P35372; entry name, OPRM\_HUMAN) onto the template produced a residue conservation profile similar to that previously obtained by us using a smaller alignment of 201 GPCR sequences.<sup>31</sup> The length of the helices was determined by considering the minimum length in the lipid bilayer, as defined by Baldwin, with subsequent addition of residues at the extracellular and intracellular limits based on sequence analysis of this region. Coordinates for the TM helices were obtained by model building ideal  $\alpha$ -helices with the appropriate kinks added to helices V and VI at P246 and P297. Side-chain conformations were determined using the backbone-dependent rotamer library of Dunbrack and Karplus.<sup>32</sup> These structures were then aligned to the  $C_\alpha$  template of Baldwin based on the orientation and vertical position of highly conserved residues across the rhodopsin family. After each addition to the TM bundle, the system was energy-minimized and equilibrated with 100 ps of restrained MD at 300 K to relieve steric contacts introduced in model building.

The model was further refined using a series of MD simulations in which positional constraints on the peptide backbone atoms were gradually reduced from 5 to 0.05 kcal/ $\text{\AA}^2/\text{mol}$ . Hydrogen-bonding distance constraints (32 kcal/ $\text{\AA}^2/\text{mol}$ ) were also imposed between the carbonyl oxygen of residue ( $i$ ) and the amide proton of residue ( $i+4$ ) to maintain an  $\alpha$ -helical conformation. Given the known problems of rhodopsin templates to capture all relevant structural data derived from functional studies of GPCRs, additional hydrogen-bonding constraints were applied to several residues to account for potential interactions. In particular, the initial  $C_\alpha$  template

places D116 and N334 more than 10  $\text{\AA}$  apart. Mutagenesis studies, however, have suggested these highly conserved residues may be part of a hydrogen-bonding network that ties together helices I (N88), II (D116), and VII (N334).<sup>33–35</sup> To account for this effect, distance constraints were added between N88, D116, and N334 during the refinement process. The entire process required approximately 700 ps of MD at 300 K. The resulting model was qualitatively evaluated for consistency with ligand binding data derived from site-directed mutagenesis data<sup>36,37</sup> and with our previous models used in docking opiates, dynorphin A, and arylacetamides.<sup>29,31</sup> All key elements of the receptor, including the highly conserved aspartate in TM-III, the cluster of aromatic residues within the receptor cavity, and the position of selectivity elements at the top of TM domains VI and VII, aligned favorably. The structural quality of the model was also verified using PROCHECK<sup>38</sup> which showed 98% of the residues in the most favored helical region and the remaining 2% in the additionally allowed helical region. Side-chain  $\chi^1$  and  $\chi^2$  angles were determined to be in their most favorable regions without stereochemical conflicts. A final energy minimization was performed on the model, which was subsequently used as the starting structure for ligand docking studies.

**Conformational Analysis.** The crystal structures of **1**,<sup>39</sup> **2**,<sup>40</sup> **4**,<sup>41</sup> **5**, and **7**<sup>42</sup> were used as starting ligand geometries, while those of **3**, **6**, and **8** were model-built from closely related X-ray structures. On the basis of the reported  $pK_a$  values of several fentanyl derivatives,<sup>16b,23</sup> the protonated form of **1–8** was considered to be the pharmacologically relevant species. The geometries of **1–8** were optimized using molecular orbital ab initio methods at the HF/6-31G\* level using the Gaussian94



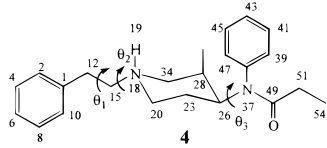
program package.<sup>43</sup> The partial atomic charges for the energy-minimized structures (**1–8**) were obtained using the restrained electrostatic potential (RESP) charge fitting formalism.<sup>44</sup> Subsequent computations of **1–8** adopted the Cornell et al. force field<sup>45</sup> (*parm94.dat* file) incorporated in AMBER 4.1 suite of programs<sup>46</sup> with appropriate additions (see Supporting Information). The ester parameters for **3** and **8** were taken from the recently published work of Kollman and co-workers.<sup>47</sup>

The MD simulations on the in vacuo energy-minimized geometries of **1–8** were performed to obtain the conformational preferences of the fentanyls in solution. Accordingly, **1–8** were placed in a periodic box of TIP3P water molecules.<sup>48</sup> Freezing the geometry of the ligand, the solvent molecules alone were energy-minimized until a rms convergence of 0.1 kcal/mol in energy was achieved. This was followed by a 5 ps equilibration of the solvent and energy minimization of the entire system (0.01 kcal/mol rms deviation in energy). A 2 ns MD simulation of the solvated ligands was then carried out at 1 atm of constant pressure. SHAKE was used to constrain bonds involving hydrogen, and the temperature of the entire system was maintained at 300 K using Berendsen algorithm<sup>49</sup> with 0.2 ps coupling constant. A 1 fs time step with an 8 Å nonbonded cutoff was also used, and the simulations were restarted every 250 ps.

**Ligand Docking.** Docking of the solution conformation of **1–8** to the model-built TM domain of the  $\mu$ -receptor was performed using the automated docking procedure (DOCK 3.5 program package)<sup>50</sup> by following the protocols described in our previous work<sup>29b</sup> and the DOCK manual. The program SPH-GEN was used to create spheres that fill the “putative ligand binding pocket” on the solvent-accessible molecular surface<sup>51</sup> of the  $\mu$ -receptor TM helices. After initial refinement of the spheres thus generated, a cluster of 43 spheres that serve as negative image descriptors was used for docking of **1–8**. A maximum of two to six bad (steric) contacts between the ligand atoms and the receptor residues were allowed while identifying potential docking configurations (orientations) in the  $\mu$ -receptor binding pocket. To find the most probable ligand alignment in the binding pocket, all predicted ligand orientations in the  $\mu$ -receptor TM domain were scored ( $E_{\text{ff}}$ , force field) individually based on the empirical evaluation of the van der Waals repulsion ( $E_{\text{rep}}$ ) and attraction ( $E_{\text{att}}$ ) and electrostatic ( $E_{\text{es}}$ ) energy contributions ( $E_{\text{ff}} = E_{\text{es}} + E_{\text{rep}} + E_{\text{att}}$ ). Site-directed mutagenesis studies on  $\mu$ -opioid ligands have shown that a D147A/D147N/D147E point mutation in TM-III of rat  $\mu$ -opioid receptor led to a diminished binding affinity,<sup>19,52</sup> presumably due to the loss of a salt bridge anchoring the receptor–ligand complex. Since the basic nitrogen in fentanyl analogues (Figure 1) is protonated under physiological conditions, ligand orientations that had this proton proximal to the TM-III aspartate (D149 in human  $\mu$ -opioid receptor) were given preference in the selection process. Consequently, the force-field scores and pharmacological results were used together to identify the most probable docking orientation in the  $\mu$ -receptor.

Refinement of the initial receptor–ligand complex was achieved by in vacuo energy minimization (0.001 kcal/mol rms deviation). A 5.0 kcal/mol positional constraint was applied to the receptor backbone atoms along with an 8 Å cutoff for nonbonded interaction. This energy-minimized complex was then subjected to an initial 250 ps MD simulation ( $\epsilon = 4$ ) with the above constraints. The force constant was subsequently reduced to 3.5 kcal/mol for the next 250 ps simulation and to 2.0 kcal/mol for the remaining 0.5 ns MD simulation. A 1 fs time step was used and the nonbonded pair list updated every 25 fs. The temperature of the system was maintained at 300 K using the Berendsen algorithm with a 0.2 ps coupling constant. Since the simulations over the last 500 ps were quite stable, the transient structure obtained from the last simulation step (1 ns) was used in the final refinement of the receptor–ligand (**1–8**) complex. With a 2 kcal/mol force constant applied for the receptor backbone atoms, the geometry optimization ( $\epsilon = 4r$ ) was terminated when the projected decrease of 0.001 kcal/mol in energy was met. Unless otherwise specified, all the docking analyses discussed hereafter are

**Table 2.** Population (%) of  $[\theta_1, \theta_2, \theta_3]$  Torsion of Fentanyl Analogues **1–8** Obtained from the 2 ns MD Simulation of the Solvated Ligands<sup>a</sup>



$[\theta_1, \theta_2]$	$[g^+, g^+]$	$[g^+, t]$	$[g^+, g^-]$	$[t, g^+]$	$[t, t]$	$[t, g^-]$	$[g^-, g^+]$	$[g^-, t]$	$[g^-, g^-]$	$\theta_3$
1	1.4	28.7	23.4	32.5	10.5	3.5	$g^+/g^-$			
2	20.8	11.6	21.5	46.2	0.1		$g^-$			
3	16.6	27.6	33.8	22.0	0.1		$g^-$			
4	48.4	6.4	9.5	34.9	0.9		$g^-$			
5	0.1		96.3	3.7			$g^-$			
6	40.6	7.7	35.0	16.8	0.1		$g^+$			
7			16.7	46.0	16.1	21.3	$g^+/g^-$			
8	0.4		59.6	24.2	13.3	2.5	$g^-$			

<sup>a</sup> *Gauche*<sup>+</sup> ( $g^+ \sim 60.0^\circ$ ), *trans* ( $t \sim 180.0^\circ$ ), *gauche*<sup>−</sup> ( $g^- \sim 300.0^\circ$ ) for  $\theta_1$  torsion. *Gauche*<sup>+</sup> ( $g^+ \sim 40.0^\circ$ ), *trans* ( $t \sim 180.0^\circ$ ), *gauche*<sup>−</sup> ( $g^- \sim 320.0^\circ$ ) for  $\theta_2$  torsion. *Gauche*<sup>+</sup> ( $g^+ \sim 150.0^\circ$ ), *cis* ( $c \sim 30.0^\circ$ ), *gauche*<sup>−</sup> ( $g^- \sim 240.0^\circ$ ) for  $\theta_3$  torsion.

based on results of the last 0.5 ns MD simulation and the subsequent minimization step.

## Results and Discussion

The relative populations of the solution structures of **1–8** are reported in Table 2. Consistent with X-ray structures,<sup>39–42</sup> spectroscopic data,<sup>53</sup> and prior computational investigations,<sup>23–27</sup> the piperidine ring favored only a chair conformation throughout the MD simulations. In addition, the methoxymethyl (**2**) and acetate (**3** and **8**) substituents to the piperidine ring were restricted mostly in the *trans* form. No preferences were noted, however, in the rotation of the terminal methyl group of the amide in **1–8**. In evaluating the remaining torsional degrees of freedom, ligand substitutions were found to have a significant impact on conformational sampling especially on  $\theta_3$  which defines the orientation of the *N*-phenylpropanamide moiety (refer to Table 2 for the definition of  $\theta_1$ – $\theta_3$  torsions). In particular, a  $\theta_3$  conformational rigidity is observed for 4- and 3-axial piperidine substitutions ( $g^-$  in **2–5**, **8**;  $g^+$  in **6**). On the other hand, an equatorial methyl substitution in **7** and the unsubstituted fentanyl (**1**) allow flexibility between the  $g^+$  and  $g^-$  forms of  $\theta_3$  and consequently are in dynamic equilibrium throughout the simulation. This equilibrium may contribute to the observed *trans* configuration of this torsion in the X-ray crystallographic structures of **1** ( $174.9^\circ$ )<sup>39</sup> and **7** ( $170.8^\circ$ ).<sup>42</sup> Using a model compound (*N*-phenyl-*N*-isopropylacetamide), the energy difference between the *trans* and  $g^{+/-}$  conformers was determined to be quite low (0.08 kcal/mol) based on ab initio Hartree–Fock (HF/6-31G\*) calculations. The X-ray structures reported may therefore represent an average of these two forms or may simply be the result of lattice packing forces in the crystal. While *cis*  $\theta_3$  conformers have been identified in a previous computational study,<sup>26</sup> this arrangement is not populated in solution due to steric crowding, especially in the piperidine 4-substituted fentanyls.

A scatter plot of the remaining  $\theta_1$  and  $\theta_2$  angles for the observed  $\theta_3$  torsions in **1–8** is given in Figure 3. These angles essentially define the overall shape of the ligand and are therefore critical to identifying the most probable “bioactive” conformation of **1–8**. An analysis

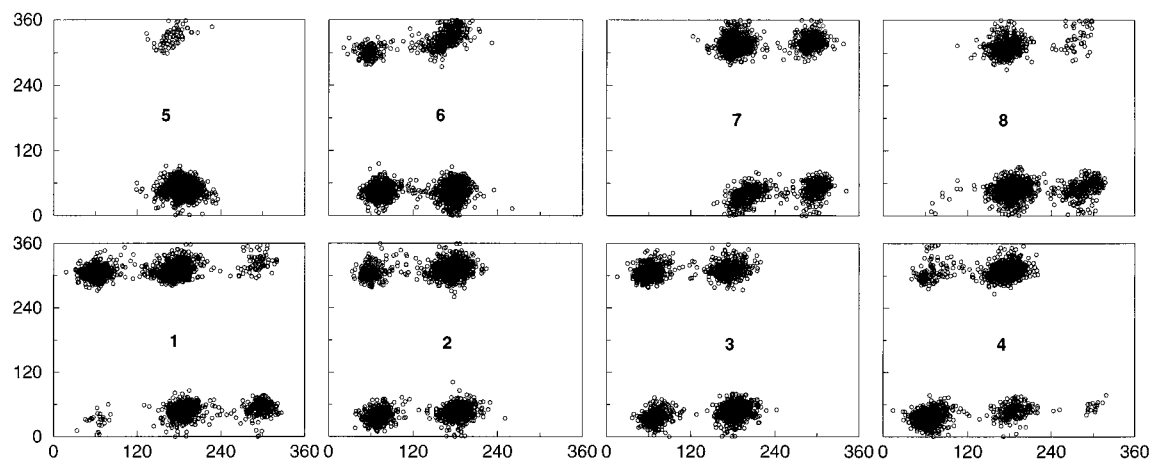


**Figure 3.** Scatter plot of the  $[\theta_1, \theta_2]$  conformational population of the solvated ligands (**1–8**) observed during the 2 ns MD simulation. Angles  $\theta_1$  (x-axis) and  $\theta_2$  (y-axis) within  $0-120^\circ \sim \text{gauche}^+$ ,  $120-240^\circ \sim \text{trans}$ , and  $240-360^\circ \sim \text{gauche}^-$ .

**Table 3.** Electrostatic ( $E_{\text{es}}$ ) and van der Waals Repulsive ( $E_{\text{rep}}$ ) and Attractive ( $E_{\text{att}}$ ) Contributions (kcal/mol) for the Best ( $E_{\text{ff}}(\text{b})$ ) and Selected ( $E_{\text{ff}}(\text{s})$ ) Docking Configuration of Various Fentanyl Analogues in the  $\mu$ -Receptor TM Domain<sup>a</sup>

no.	starting conformer for docking $[\theta_1, \theta_2, \theta_3]$	$E_{\text{ff}}(\text{b})$			$E_{\text{ff}}(\text{s})$			populated conformer in complex $[\theta_1, \theta_2, \theta_3]$	%
		$E_{\text{es}}$	$E_{\text{rep}}$	$E_{\text{att}}$	$E_{\text{es}}$	$E_{\text{rep}}$	$E_{\text{att}}$		
<b>1</b>	$[t, g^-, g^+]$	−3.7	13.6	−33.9	0.3	31.8	−39.5	$[g^-, g^-, g^-]$	74.6 <sup>b</sup>
<b>2</b>	$[t, g^-, g^-]$	−3.8	15.6	−36.0	−3.5	15.0	−34.9	$[t, g^-, g^-]$	85.6
<b>3</b>	$[t, g^+, g^-]$	−3.2	12.3	−32.7	−1.7	47.9	−44.8	$[t, g^-, g^-]$	80.6
<b>4</b>	$[t, g^-, g^-]$	−2.4	12.7	−34.6	−10.2	61.8	−60.9	$[t, g^-, g^-]$	97.2
<b>5</b>	$[t, g^+, g^-]$	−4.8	15.1	−34.9	−3.0	36.3	−48.7	$[t, g^-, g^-]$	81.6
<b>6</b>	$[t, g^+, g^+]$	−0.9	22.8	−47.4	−7.7	89.8	−69.5	$[g^-, g^+, g^+]$	90.0
<b>7</b>	$[t, g^-, g^+]$	−4.0	18.6	−39.6	−8.4	92.6	−75.5	$[t, g^-, g^-]$	99.4
<b>8</b>	$[t, g^+, g^-]$	−3.2	10.2	−29.4	−10.5	214.0	−77.4	$[t, g^+, g^-]$	99.2

<sup>a</sup> The last two columns represent the dominant ligand conformation and its population (in %) in the  $\mu$ -receptor obtained from the last 0.5 ns MD simulation. <sup>b</sup>  $[t, g^-, g^-]$  conformer is 22.8% populated.

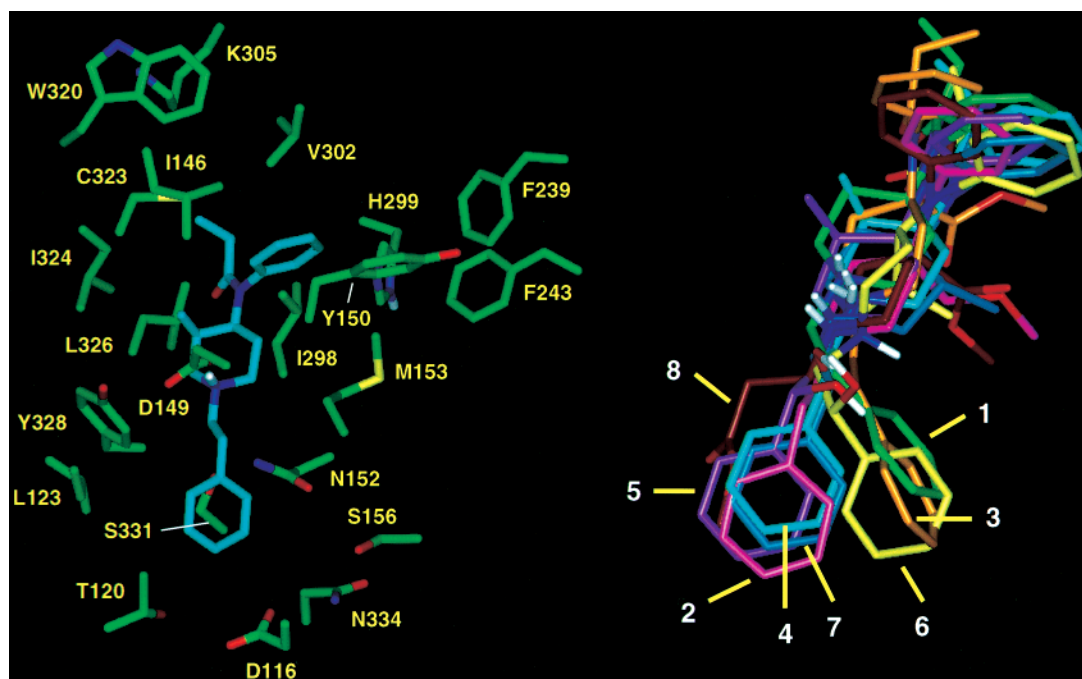
of this plot indicates the *trans* or extended  $\theta_2$  torsion is not populated in solution. Except for **1**, **7**, and **8**, the  $[g^-, g^-, \theta_3]$  orientation is not sampled in the MD run and the  $[g^-, g^+, \theta_3]$  arrangements are scarcely populated. Discarding the conformers that are <5% populated in solution for **1–8**, a maximum of 4 conformers are sampled in solution out of the 27 conformational possibilities (3-fold rotation around each  $\theta$ ). However, their relative populations vary across the series (Table 2) and reveal different conformational preferences for each ligand. For instance, the  $[t, g^-, g^-]$  X-ray structure<sup>40</sup> is also the highly populated (46%) solution structure for **2**, while the  $[t, g^-, g^-]$  crystal structure orientation of *cis*-3-methylfentanyl<sup>41</sup> is the second most populated (35%) isomer observed for the solvated species. The most potent ohmefentanyl derivative, **5**, exists in the  $[t, g^+, g^-]$  X-ray structure<sup>42</sup> orientation and is conformationally rigid with 96% populated in solution. In contrast, the inactive enantiomer (**6**) is flexible with the  $[g^+, g^+, g^+]$  and  $[t, g^+, g^+]$  isomers sampled around 35% and the  $[t, g^-, g^+]$  isomer populated by 17% (Table 2). Although the chirality (3*R*,4*S*) is the same, the solution conformer of **4** differs significantly in the preference for  $\theta_1$  and  $\theta_2$  torsions as compared to **5**. A striking observation of the MD simulations, however, is the strong preference for *trans* and *gauche*<sup>−</sup>  $\theta_1$  and  $\theta_3$  torsions, respectively, for most of the active ligands, while the *gauche*<sup>+</sup>  $\theta_3$  torsion dominates the weakly bound ligand **6**.

Table 3 lists the initial conformations of **1–8** used in automated docking as well as the resulting DOCK force-field scores. Although priority was given to the most highly populated solution structures in docking, incon-

sistencies were noted in the binding modes of **4** and **6** when compared with the remainder of the ligands in the series.<sup>54</sup> This was addressed by selecting the second most populated solution structure for these ligands. Automated docking of this revised set of conformations to the TM domain of the  $\mu$ -opioid receptor resulted in several (~50 to ~215) plausible docking orientations for each ligand. In the process of evaluating these docking configurations using the force-field scores, we found the best overall scored binding modes did not always correlate with the results from site-directed mutagenesis studies.<sup>52a</sup> Except for **2**, none of the best scored docking orientations had the protonated nitrogen of the piperidine ring close to D149 in TM-III.

The origin of this disparity can be traced to the components of the DOCK scores. In comparing the best scored orientations with those that contain the key D149 ligand contact, significant differences are noted in the repulsive component of the score (Table 3). For all ligands (except **2**), the repulsive energy dominates the score of the D149-bound orientations. This problem is most likely due to uncertainties in the side-chain conformation of the model-built receptor but may also stem from limitations in the use of rigid docking protocols. Table 3 therefore lists the overall best scored docking orientation as well as the selected orientations that account for the key D149–ligand contact.

Finally, the sensitivity of the docking orientation and the conformation of the initial receptor–ligand complex were verified by performing additional MD simulations for fentanyl starting from a different ligand docking orientation ( $E_{\text{ff}}(\text{s}) = [-0.7, 33.8, -40.4]$ ) and for carfen-



**Figure 4.** Key residues surrounding *cis*-3-methylfentanyl (**4**) in the  $\mu$ -receptor binding pocket (left). A superposition of **1–8** in the  $\mu$ -receptor binding pocket is shown on the right.

tanil starting with a different ligand conformation ( $[t, g^-, g^-]$ ). Irrespective of the starting receptor–ligand geometry, the MD simulations of both the complexes resulted in final configurations that were similar to the ones reported in Table 3.

The MD trajectories of the receptor–ligand complexes indicate the fentanyl analogues align diagonally across the receptor cavity, spanning TM-II, -III, -VI, and -VII. A depiction of the ligand binding mode and superposition of the bound conformations of **1–8** is given in Figure 4. This binding site model is supported by ligand binding studies to  $\mu/\kappa$  and  $\mu/\delta$  chimera that have shown TM-I–III, -VI, and -VII are essential to sufentanil binding.<sup>18</sup> The proposed docking orientation places the *N*-phenylpropanamide group toward the extracellular side of the cavity (between TM-III and -VI), while the *N*-phenethyl group slides through TM-III and -VII toward the intracellular end of the cavity. A detailed examination of the binding modes for **1–8**, however, reveals some differences in the orientation of these functional groups across the series. In the case of the *N*-phenethyl group, differences are noted in the binding of **1**, **6**, and **8** as compared to that of **2–5** and **7**. More specifically, the phenethyl group of **2–5** and **7** is projected toward TM-II while the same moiety is directed toward TM-III in **1**, **6**, and **8** (Figure 4). As a result, the receptor–ligand complexes of **2–5** and **7** gain additional stabilization from residues in TM-II and -VII. These subtle differences in the ligand conformations may be a contributing factor in reducing the affinity of **5** (by 590-fold) to a  $\kappa/\mu$  chimeric receptor in which TM-I and -II are taken from  $\kappa$  and TM-III–VII are taken from  $\mu$ .<sup>21</sup> The binding affinity of **6**, on the other hand, was effected much less (40-fold), lending support to the hypothesis. Similarly, the proximity of the phenethyl group of **1** to TM-III, and especially to N150 (which appears to sterically hinder binding), is corroborated by the 20-fold increase observed in fentanyl binding upon

**Table 4.** Selected Residues within 5 Å Surrounding the Various Functional Moieties of **1–8** in the TM Domain of the  $\mu$ -Receptor Binding Pocket ( $\mu$ -receptor-specific residues are underlined)

helix no.	residue no. in the $\mu$ -receptor
TM-II	(T120, <u>L123</u> ) <sup>a</sup> , T122 <sup>b</sup>
TM-III	(N152 <sup>b</sup> , M153) <sup>a</sup> , ( <u>I146</u> , D149) <sup>b,c</sup> , Y150 <sup>d</sup> , S156 <sup>a</sup>
TM-V	(F239, F243) <sup>d</sup>
TM-VI	I298 <sup>c</sup> , H299 <sup>d</sup> , (V302, K305) <sup>e</sup>
TM-VII	(N330, S331 <sup>b</sup> , N334, P335) <sup>a</sup> , (G327, Y328) <sup>b,c</sup> , ( <u>W320</u> , C323, I324, L326) <sup>e</sup>

<sup>a</sup> Residues close to the *N*-phenethyl moiety. <sup>b</sup> Residues close to the 2'-OH substituent in **5–7**. <sup>c</sup> Residues close to the piperidine ring. <sup>d</sup> Residues close to the *N*-phenyl ring. <sup>e</sup> Residues close to O=C–C<sub>2</sub>H<sub>5</sub>.

a N150A point mutation.<sup>20a</sup> A listing of residues proximal to the *N*-phenethyl group in **1–8** can be found in Table 4.

The position of the *N*-phenylpropanamide group is of particular interest. This group is directed toward the top of TM-VI which contains key recognition elements in the binding of several opioid ligands. In particular, position VI:23 (K305; Figure 2) has been identified in the binding and selectivity of the rigid  $\mu$ -opioids such as norBNI<sup>55</sup> and GNTI<sup>56</sup> (E297 in  $\kappa$ ) and the  $\delta$ -selective piperazine derivative SNC80<sup>57</sup> (W284 in  $\delta$ ). A comparison of the binding modes of **1–8** in this domain shows the *N*-phenylpropanamide group of **1–7** adopts a similar arrangement between TM-III and -VI. However, the fentanyl skeleton is simply too small to span the receptor cavity (i.e. D149–K305) and consequently cannot extend up to the similarly placed  $\mu$ -specific residue, K305. This tends to rule out this position in conferring selectivity of **1–8** and suggests different elements may drive the molecular recognition process at the  $\mu$ -receptor.

An analysis of the residues flanking the remaining functional groups also reveals some ligand-specific differences. Perhaps the most provocative involves the



key D149 salt link. This interaction has been shown to be a key anchor to recognition and binding of a number of opioid ligands, including peptides, rigid opiates, and nontypical opioids such as U50,488.<sup>19,58</sup> The MD simulations of the receptor–ligand complexes, however, indicate this salt link is lost in one case. Although each ligand–receptor complex was started with this contact intact, the orientation of **6** changed within the first 100 ps breaking this critical link. This appears to be due to the  $g^+$   $\theta_3$  torsion of **6** that orients the 3-methyl group much closer to M153 in the initial complex (note that the same torsion is  $g^-$  in **5** and **7**; Table 3). Similarly, the *N*-phenyl group encounters steric clashes with I298 and I324 as does the *N*-phenethyl group with A119 and Y328. Hindered by repulsive interactions with the receptor, the ligand realigns during the simulation disrupting the salt bridge. As a result, the 2'-OH group of **6** is close to hydrogen-bonding distance with the carboxylate group of D149. This may, in part, explain the reduced binding affinity of **6** compared to other members in the ohmefentanyl series.<sup>14</sup>

Ligand-specific differences are also noted in the receptor interactions with substituents on the piperidine ring (**2**, **3**). Although docked close to H299 in TM-VI, the polar substituents of this ring are not positioned appropriately to take advantage of donor–acceptor interactions with the imidazole side chain of this residue, suggesting that H299 is not directly involved in fentanyl binding. This general hypothesis is supported by ligand binding studies that indicate sufentanil binding remains unaffected by H297N or H297Q point mutations in the rat  $\mu$ -opioid receptor.<sup>59</sup> The axial 3-methyl substitutions in **4** and **5** are ideally placed to benefit from hydrophobic interactions with residues in TM-III and -VII, while the equatorial methyl group of **7** points to a domain between TM-III and -V.

Although such differences in hydrophobic interactions with the receptor may be an important factor contributing to the differential binding of **5** and **7**, these ligands also contain a 2'-hydroxyl group that may attenuate affinity. In fact, the hydroxyl group of **5** and the hydroxyl group of S331 come in close contact during some stages of the MD simulation, providing an additional anchor point to receptor–ligand association. A similar interaction is possible for the hydroxyl group of T122 and the 2'-OH of **5** and **7**. It is important to point out, however, that an alternative docking arrangement has been proposed for ohmefentanyl. Tang et al. hypothesized that this hydroxyl may form a hydrogen bond with Y150.<sup>60</sup> While Xu et al.<sup>61</sup> have reported a reduction in binding affinity of **5** and **6** to a Y150F mutant  $\mu$ -receptor (Y148 in rat sequence), the effect is marginal (4–7-fold) which casts some doubt over the interpretation. Similar reductions in affinity have been noted for other residues in the cavity of opioid receptors that are not directly involved in ligand binding. Nevertheless, the alternative docking arrangement for the 2'-OH cannot be ruled out at this point in time.

The docking mode(s) proposed here is also consistent with SAR data reported for a number of fentanyl derivatives. As seen in Figure 4, positions  $\alpha$  to the basic nitrogen in fentanyl dock between TM-III and -VII in a fairly restricted binding domain. Substitutions to the  $\alpha$  position may therefore encounter steric repulsions with

the receptor side chains, thereby disrupting the salt link with D149. This may explain the dramatic loss in activity observed for 2,3-, 2,5-, and 3,5-dimethylpiperidine ring derivatives of fentanyl.<sup>62</sup> Similarly, the proximity of the 3-methyl substitution in **4** and **5** to G327 (TM-VII) is consistent with the diminished binding affinities observed for 3-allyl- and 3-propylpiperidine substitutions.<sup>63</sup> In general, SAR studies suggest relatively small, planar fragments as favored terminal groups to the ethyl spacer. Thus, constrained derivatives,<sup>64</sup> which include benzo-fused heteropentacycles and other bicyclic derivatives, show a marked reduction in binding affinity (ca. 300-fold) when compared to **1**.<sup>65</sup> While cyclization increases steric bulk in this region of the ligand, it also restricts the  $\theta_1$  and  $\theta_2$  angles that define critical recognition elements. The results reported here suggest the most strongly bound ligands prefer an extended or *trans*  $\theta_1$ . Cyclization may, in effect, lock the structure in a less than optimal conformation, leading to an overall decrease in binding affinity. These same arguments could be extended to explain the decreased affinity of cyclized derivatives of the *N*-phenylpropanamide and piperidine rings.<sup>66</sup> The *N*-phenyl ring of **1–8** is close to a number of side-chain residues in TM-III. Cyclization may therefore produce steric hindrance and crowding of the ligand in this region. The position of the phenyl ring in this local binding domain is further supported by SAR data on *ortho/para/meta* substitutions.<sup>6b</sup> Whereas the *ortho* positions of the *N*-phenyl ring lie close to residue side chains in TM-III, the *meta* and *para* positions project between TM-III and -VI. This is consistent with the reduction in binding affinity reported for fentanyl derivatives that contain bulky groups *ortho* to the *N*-phenyl bond.<sup>6</sup>

As a final test of the docking mode(s) proposed for **1–8**, the bound conformation of **4** was compared with that of a previous binding site model reported for opiates.<sup>31</sup> One opiate, in particular, has significant relevance to the evaluation of fentanyl docking. The addition of an *N*-phenethyl group to normorphine has been shown to increase the potency at the  $\mu$ -receptor.<sup>67</sup> The resulting compound, *N*-phenethylnormorphine (**10**), contains the key *N*-phenethyl group typically associated with fentanyl activity. To evaluate potential connections between these ligand classes, **10** was docked similar to **1–8** and subsequently overlaid with the bound conformation of fentanyl (**1**). A comparison of the positions of these ligands is given in Figure 5. A detailed examination of the docked structures indicates the cationic amines of both ligand classes align and interact similarly with D149 through salt bridge formation. Moreover, the *N*-phenethyl groups show substantial overlap and project into the same binding domain in the  $\mu$ -receptor. Considering the overall differences in the structures of these ligand classes, the result is highly provocative and provides additional support for the binding mode proposed here for fentanyl. In contrast, no overlap is apparent between the aromatic groups of **4** and the phenolic moiety of the opiate. This is due to the disposition of the aromatic substituents with respect to the axial or equatorial positions of the piperidine ring (Figure 5). Consequently, the phenolic ring in **10** projects deep into the receptor cavity toward a cluster of aromatic residues flanked by TM-III and -V (see ref

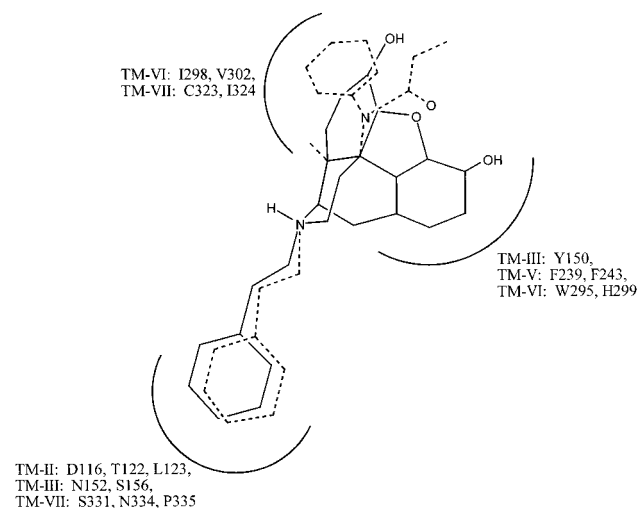


**Figure 5.** Superposition of *cis*-3-methylfentanyl (**4**; dashed) and *N*-phenethylnormorphine (**10**; solid), showing potential residue contacts of both ligands.

31 for a detailed discussion of opiate docking). While site-directed mutagenesis studies have implicated several of these aromatic residues in binding opiates, it is important to point out that similar results have not surfaced to link fentanyl-based ligands to this binding domain in the  $\mu$ -receptor. This lends some support to the relative disposition of the aromatic rings shown in Figure 5.

## Conclusions

This study has presented a binding site model for a series of fentanyl derivatives using a combination of solution-phase conformational analysis and automated docking techniques. One of the more interesting results of the work regards the potential relationship observed between ligand conformation and binding affinity. The results of the solution-phase dynamics calculations suggest that the most potent fentanyl derivatives possess an extended conformation for the phenethyl group with  $\theta_1 = \text{trans}$  and  $\theta_2 = \text{gauche}$ . This suggests that minor differences in the conformations of substituted fentanyls may have a significant impact on ligand binding. Given the close structural relationship of **1**–**7**, this outcome was unexpected at the outset of our study. Support for this conclusion can be found in the reduced affinity of **6** (which adopts a more compact form) and the diminished activity of cyclized derivatives that lock the torsions in less than optimal values.<sup>64,65</sup> This may also explain the differences in binding modes reported by Pogozheva et al.<sup>22</sup> with that reported here for **4** (*cis*-3-methylfentanyl). The conformation selected for docking in that study possessed  $\theta_1$  and  $\theta_2$  torsion angles of 282° and 201°, respectively. This structure, however, was not populated during our solution-phase simulations. This is true of all fentanyl derivatives with a *trans*  $\theta_2$  which are predicted to be higher in energy when compared with the corresponding *gauche* forms. In fairness to Pogozheva et al.,<sup>22</sup> it is important to point out that the focus of their study was on receptor structure, and not directed to a detailed analysis of fentanyl and fentanyl derivatives. Nevertheless, it is clear that conformer selection has a significant impact on the predicted binding mode. Taken overall, this

indicates great care must be taken in evaluating the conformational properties of all ligand derivatives, regardless of the close structural relationships displayed across a given series.

The automated ligand docking results have also led to the development of a unique binding site model for fentanyl that explains available pharmacological data as well as SAR data for a number of fentanyl derivatives. To date, most models of opioid recognition place the ligand in a main cavity of the receptor formed by TM-III–VII. This cavity is essentially bounded by the conserved Asp in TM-III (D149) and a cluster of aromatic residues in TM-V and -VI. The docking mode proposed here, however, places the *N*-phenethyl group of fentanyl deep in a crevice between TM-II and -III with the *N*-phenylpropanamide moiety projected diagonally toward TM-VI and -VII. This also aligns the cationic amine of fentanyl with D149 but leaves the aromatic pocket of the receptor unoccupied. While the model is generally supported by ligand binding data to  $\mu/\kappa$  chimeras,<sup>18</sup> the most convincing evidence can be found in Figure 5. A comparison of the binding modes of *cis*-3-methylfentanyl and *N*-phenethylnormorphine (**10**) indicates the phenethyl groups project into the same binding domain in the  $\mu$ -receptor, despite clear differences in the overall binding modes of the ligands. (Note the phenolic moiety of the opiate is bound in the aforementioned aromatic pocket of the cavity.) These results suggest that the  $\mu$ -receptor may contain an important recognition site relatively deep into the receptor cavity between TM-II and -III. The significance of such a conclusion is further heightened by the finding that changes in TM-II may be linked with receptor activation and high/low-affinity binding of agonists. A single mutation of D116 (D114 in rat) has been shown to constitutively deactivate opioid receptors, leading to a decrease in agonist affinity.<sup>68</sup> The interaction of the *N*-phenethyl ring of fentanyl (and the opiate) with TM-II may therefore play some role in receptor activation. Although this is highly speculative, steric interactions between the retinal chromophore and TM-III of rhodopsin have been shown to trigger signal transduction.<sup>69</sup>

The results of this study have further provided insight to potential targets for site-directed mutagenesis studies and the design of novel fentanyl derivatives. Such experiments not only are critical to evaluating the binding site model proposed but also are of great importance to understanding the structural basis to selectivity for this ligand class. For example, mutation of S331 may help define the orientation of the phenethyl ring within the receptor cavity. This residue is a potential hydrogen-bonding partner with the 2'-OH of the ohmefentanyl derivatives. The comparison with the opiate is especially enlightening and shows additional steric bulk can be accommodated in the 4-axial position of the piperidine ring. Although 4-phenyl/heteroaryl substitutions have been shown to improve analgesic potency at the  $\mu$ -receptor,<sup>70</sup> the effect of incorporating a phenolic group in this position has not been tested. It may be of particular interest to examine the effect of mutating H299 on the binding of such derivatives as this residue has been linked with opiate binding<sup>59</sup> (but not with fentanyl). The overlap noted in the *N*-phenethyl groups of the opiate and **4** is also suggestive. Substitu-



tion of this position in opiates is known to convert agonists to antagonists and vice versa (e.g. oxymorphone/naloxone/naltrexone). Given the results of Figure 5, it may therefore be of value to examine the effect of substituting the *N*-phenethyl group of (ohme)fentanyl with an allyl (as in naloxone) or cyclopropylmethyl (as in naltrexone).<sup>2c</sup> Such experiments may lead to the characterization of a hitherto unknown fentanyl-based antagonist that may be of extreme value as a pharmacological tool and for the development of analgesics with modified properties.

Finally, it is important to emphasize that ligand binding studies have not yet determined key selectivity sites for nonpeptide ligands in the  $\mu$ -receptor. In sharp contrast, site-directed mutagenesis studies have located specific residues near the extracellular boundary of TM-VI and -VII that are involved in ligand selectivity in both the  $\delta$ - and  $\kappa$ -receptors.<sup>55,57</sup> Albeit indirectly, this suggests the recognition process at the  $\mu$ -receptor may be unique. In reviewing the results of this study and those of others, it is clear that the selectivity of fentanyl cannot be explained by close proximity of a single residue (as in  $\kappa$  or  $\delta$ ) but appears to be more dependent on a number of  $\mu$ -specific contacts within the receptor. The structural basis to fentanyl binding may therefore be related to subtle differences in the steric makeup or conformation of the opioid receptors which may or may not be related to the high/low-affinity binding states. This may also cause fentanyl to adopt different binding modes in the  $\mu$ -,  $\delta$ -, and  $\kappa$ -receptors. While this adds another dimension to the design and interpretation of structure-based experiments (including mutational studies, ligand design, and molecular modeling), it may explain the difficulties encountered in developing models of recognition for the  $\mu$ -receptor. The results of this study strongly suggest the binding domain surrounding the *N*-phenethyl group may be an excellent starting point to explore this phenomenon. Given the recent success reported in modulating the selectivity of opiates based on  $\kappa$ - and  $\delta$ -models of recognition,<sup>56</sup> the resolution of problems in determining  $\mu$ -receptor binding and selectivity may ultimately lead to the rational design of ligands for all three opioid subtypes.

**Acknowledgment.** The authors thank NIH/NIDA for financial support to D.M.F., P.S.P., and M.G.P.

**Supporting Information Available:** Force-field parameters and experimental pharmacological data used in this study along with the in vacuo geometry-optimized coordinates (PDB format) and RESP partial atomic charges of **1–8** and **10** and also the putative ligand binding pocket in the  $\mu$ -receptor TM domain and the binding orientations of **1–8** and **10** obtained from 1 ns MD simulation of the receptor–agonist complex. This material is available free of charge via the Internet at <http://pubs.acs.org>.

## References

- Janssen, P. A. J. A Review of the Chemical Features Associated with Strong Morphine-like Activity. *Br. J. Anaesth.* **1962**, *34*, 260–268.
- (a) Helsley, G. C.; Lunsford, C. D.; Welstead, W. J., Jr.; Boswell, R. F.; Funderburk, W. H.; Johnson, D. N. Synthesis and Analgesic Activity of Some 1-substituted 3-pyrrolidinylanilides and dihydrobenzoxazinones. *J. Med. Chem.* **1969**, *12*, 583–586. (b) van Bever, W. F. M.; Niemegeers, C. J. E.; Janssen, P. A. J. Synthetic Analgesics. Synthesis and Pharmacology of the Diastereoisomers of *N*-[3-Methyl-1-(2-phenethyl)-4-piperidyl]-*N*-phenylpropanamide and *N*-[3-Methyl-1-(1-methyl-2-phenylethyl)-4-piperidyl]-*N*-phenylpropanamide. *J. Med. Chem.* **1974**, *17*, 1047–1051. (c) Finney, Z. G.; Riley, T. N. 4-Anilidopiperidine Analgesics. 3. 1-Substituted 4-(Propananilido)perhydroazepines as Ring-Expanded Analogues. *J. Med. Chem.* **1980**, *23*, 895–899. (d) Borne, R. F.; Law, S.-Y.; Kapeghian, J. C.; Masten, L. W. Evaluation of 2-Azabicyclo[2.2.2]octane Analogues of 4-Anilidopiperidine Analgesics. *J. Pharm. Sci.* **1980**, *69*, 1104–1106. (e) Maryanoff, B. E.; Simon, E. J.; Gioannini, T.; Gorissen, H. Potential Affinity Labels for the Opiate Receptor Based on Fentanyl and Related Compounds. *J. Med. Chem.* **1982**, *25*, 913–919. (f) Fernandez, M. J.; Huertas, R. M.; Galvez, E.; Orjales, A.; Berisa, A.; Labeaga, L.; Gago, F.; Fonseca, I.; Sanz-Aparicio, J.; Cano, F. H.; Albert, A.; Fayor, J. Synthesis, and Structural, Conformational and Pharmacological Studies of New Fentanyl Derivatives of the Norgranatane System. *J. Chem. Soc., Perkin Trans. 2* **1992**, 687–695.
- (a) Martin, W. R. Pharmacology of Opioids. *Pharmacol. Rev.* **1983**, *35*, 283–323. (b) Millan, M. J. Multiple Opioid systems and Pain. *Pain* **1986**, *27*, 303–347. (c) Lenz, G. R.; Evans, S. M.; Walters, D. E.; Hopfinger, A. J. *Opiates*; Academic Press: New York, 1986. (d) Jaffe, J. H.; Martin, W. R. Opioid Analgesics and Antagonists. In *The Pharmacological Basis of Therapeutics*, 8th ed.; Gilman, A. G., Rall, T. W., Nies, A. S., Taylor, P., Eds.; Pergamon Press: New York, 1990; pp 485–521. (e) Raynor, K.; Kong, H.; Chen, Y.; Yasuda, K.; Yu, L.; Bell, G. I.; Reisine, T. Pharmacological Characterization of the Cloned  $\kappa$ -,  $\delta$ -, and  $\mu$ -opioid Receptors. *Mol. Pharmacol.* **1994**, *45*, 330–334. (f) Satoh, M.; Minami, M. Molecular Pharmacology of the Opioid Receptors. *Pharmacol. Ther.* **1995**, *68*, 343–364. (g) Kieffer, B. L. Recent Advances in Molecular Recognition and Signal Transduction of Active Peptides: Receptors for Opioid Peptides. *Cell. Mol. Neurobiol.* **1995**, *15*, 615–635. (h) Dhawan, B. N.; Cesselin, F.; Raghunir, R.; Reisine, T.; Bradley, P. B.; Portoghese, P. S.; Hamon, M. International Union of Pharmacology. XII. Classification of Opioid Receptors. *Pharmacol. Rev.* **1996**, *48*, 567–592.
- (a) Colapet, J. A.; Diamantidis, G.; Spencer, H. K.; Spaulding, T. C.; Rudolph, F. G. Synthesis and Pharmacological Evaluation of 4,4-Disubstituted Piperidines. *J. Med. Chem.* **1989**, *32*, 968–974. (b) France, C. P.; Winger, G.; Madzihradsky, F.; Seggel, M. G.; Rice, K. C.; Woods, J. H. Mirfentanil: Pharmacological Profile of a Novel Fentanyl Derivative with Opioid and Nonopioid Effects. *J. Pharmacol. Exp. Ther.* **1991**, *258*, 502–510. (c) France, C. P.; Gerak, L. R.; Flynn, D.; Winger, G. D.; Madzihradsky, F.; Bagley, J. R.; Brockunier, L. L.; Woods, J. H. Behavioral Effects and Receptor Binding Affinities of Fentanyl Derivatives in Rhesus Monkeys. *J. Pharmacol. Exp. Ther.* **1995**, *274*, 17–28.
- Strand, F. L. *Neuropeptides: Regulators of Physiological Processes*; MIT Press: Cambridge, 1999; Chapter 14 and references therein.
- (a) Lobbezoo, M. W.; Soudijn, W.; van Wijngaarden, I. Structure and Receptor Interactions of Morphinomimetics. Part I. Hydroxy and Methoxy Derivatives of Fentanyl and some Morphine Analogues. *Eur. J. Med. Chem. – Chim. Ther.* **1980**, *15*, 357–361. (b) Lobbezoo, M. W.; Soudijn, W.; van Wijngaarden, I. Opiate Receptor Interaction of Compounds Derived from or Structurally Related to Fentanyl. *J. Med. Chem.* **1981**, *24*, 777–782.
- (a) Casy, A. F.; Hassan, M. M. A.; Simmonds, A. B.; Staniforth, D. Structure–activity Relations in Analgesics Based on 4-anilidopiperidine. *J. Pharm. Pharmacol.* **1969**, *21*, 434–440. (b) Maguire, P.; Tsai, N.; Kamal, J.; Cometta-Morini, C.; Upton, C.; Loew, G. Pharmacological Profiles of Fentanyl Analogues at  $\mu$ ,  $\delta$  and  $\kappa$  Opiate Receptors. *Eur. J. Pharmacol.* **1992**, *213*, 219–225.
- Feldman, P. L.; James, M. K.; Brackeen, M. F.; Bilotta, J. M.; Schuster, S. V.; Lahey, A. P.; Lutz, M. W.; Johnson, M. R.; Leighton, H. F. Design, Synthesis, and Pharmacological Evaluation of Ultrashort- to Long-Acting Opioid Analgesics. *J. Med. Chem.* **1991**, *34*, 2202–2208 and references therein.
- van Bever, W. F. M.; Niemegeers, C. J. E.; Schellekens, K. H. L.; Janssen, P. A. J. *N*-4-Substituted 1-(2-Arylethyl)-4-piperidyl-*N*-phenylpropanamides, a Novel Series of Extremely Potent Analgesics with Unusually High Safety Margin. *Arzneim-Forsch.* **1976**, *26*, 1548–1551.
- van Daele, P. G. H.; DeBruyn, M. F. L.; Boey, J. M.; Sanczuk, S.; Agten, J. T. M.; Janssen, P. A. J. Synthetic Analgesics: *N*-(1-[2-Arylethyl]-4-substituted 4-piperidyl) *N*-Arylalkanamides. *Arzneim-Forsch.* **1976**, *26*, 1521–1526.
- Wang, Z.-X.; Zhu, Y.-C.; Chen, Z.-J.; Ji, R.-Y. Stereoisomers of 3-Methylfentanyl: Synthesis, Absolute Conformation and Analgesic Activity. *Acta Pharm. Sin.* **1993**, *28*, 905–910.
- (a) Band, L.; Xu, H.; Bykov, V.; Greig, N.; Kim, C.-H.; Newman, A.; Jacobson, A. E.; Rice, K. C.; Rothman, R. B. The Potent Opioid Agonist, (+)-*cis*-3-Methylfentanyl Bind Pseudoirreversibly to the Opioid Receptor Complex in vitro and in vivo: Evidence for a Novel Mechanism of Action. *Life Sci.* **1990**, *47*, 2231–2240. (b) Xu, H.; Kim, C.-H.; Zhu, Y. C.; Weber, R. J.

- Jacobson, A. E.; Rice, K. C.; Rothman, R. B. (+)-*cis*-3-Methylfentanyl and its Analogues Bind Pseudoirreversibly to the Mu Opioid Binding Site: Evidence for Pseudoallosteric Modulation. *Neuropharmacology* **1991**, *30*, 455–462.
- (13) Jin, W.-Q.; Xu, H.; Zhu, Y.-C.; Fang, S.-N.; Xia, X.-L.; Huang, Z.-M.; Ge, B.-L.; Chi, Z.-Q. Studies on Synthesis and Relationship Between Analgesic Activity and Receptor Affinity for 3-Methylfentanyl Derivatives. *Sci. Sin.* **1981**, *24*, 710–720.
- (14) (a) Xu, H.; Jie, C.; Chi, Z.-Q. Ohmefentanyl – A New Agonist for  $\mu$ -opioid Receptor. *Sci. Sin.* **1985**, *28*, 504–511. (b) Brine, G. A.; Stark, P. A.; Carroll, F. I.; Xu, H.; Rothman, R. B. Enantiomers of ( $\pm$ )-*cis*-N-[1-(2-Hydroxy-2-phenylethyl)-3-methyl-4-piperidyl]-N-phenylpropanamide Influence of the Hydroxyl Group. *Med. Chem. Res.* **1992**, *2*, 34–40. (c) Ni, Q.; Xu, H.; Partilla, J. S.; Stark, P. A.; Carroll, F. I.; Brine, G. A.; Rothman, R. B. Stereochemical Requirements for Pseudoirreversible Inhibition of Mu Receptor Binding by the 3-Methylfentanyl Congeners, RTI-46144 and its Enantiomers: Evidence for Different Binding Domains. *Synapse* **1993**, *15*, 296–306. (d) Wang, Z.-X.; Zhu, Y.-C.; Chen, X.-J.; Ji, R.-Y. Ohmefentanyl Enantiomers and its Analgesic Activity. *Chin. Sci. Bull.* **1994**, *9*, 2004–2008. (e) Wang, Z.-X.; Zhu, Y.-C.; Jin, W.-Q.; Chen, X.-J.; Chen, J.; Ji, R.-Y.; Chi, Z.-Q. Stereoisomers of N-[1-(2-Hydroxy-2-phenylethyl)-3-methyl-4-piperidyl]-N-phenylpropanamides: Synthesis, Stereochemistry, Analgesic Activity, and Opioid Receptor Binding Characteristics. *J. Med. Chem.* **1995**, *38*, 3652–3659. (f) Lu, Y.-F.; Xu, H.; Partilla, J. S.; Brine, G. A.; Carroll, F. I.; Rice, K. C.; Sadee, W.; Rothman, R. B. Opioid Peptide Receptor Studies. 5. Further Evidence that the Methylfentanyl Congener RTI-4614-4 and its Four Stereoisomers Bind to Different Domains of the Rat  $\mu$ -opioid Receptor. *Analgesia* **1996**, *2*, 291–297. (g) Xu, H.; Lu, Y.-F.; Partilla, J. S.; Brine, G. A.; Carroll, F. I.; Rice, K. C.; Lai, J.; Porreca, F.; Rothman, R. B. Opioid Peptide Receptor Studies. 6. The 3-Methylfentanyl Congeners RTI-4614-4 and its Enantiomers Differ in Efficacy, Potency, and Intrinsic Efficacy as Measured by Stimulation of [ $^{35}$ S]GTP- $\gamma$ -S Binding Using Cloned  $\mu$ -opioid Receptors. *Analgesia* **1997**, *3*, 35–42.
- (15) (a) Niemegeers, C. J. E.; Schellekens, K. H. L.; van Bever, W. F. M.; Janssen, P. A. J. Sufentanil, a very Potent and Extremely Safe Intravenous Morphine-like Compound in Mice, Rats, and Dogs. *Arzneimittelforsch.* **1976**, *26*, 1551–1556. (b) Monk, J. P.; Beresford, R.; Ward, A. Sufentanil: A Review of its Pharmacological Properties and Therapeutic Use. *Drugs* **1988**, *36*, 286–313.
- (16) (a) James, M. K.; Feldman, P. L.; Schuster, S. V.; Bilotta, J. M.; Brackeen, M. F.; Leighton, H. J. Opioid Receptor Activity of GI 87084B, A Novel Ultra-short Acting Analgesic in Isolated Tissues. *J. Pharmacol. Exp. Ther.* **1991**, *259*, 712–718. (b) Glass, P. S. A. Remifentanyl: A New Opioid. *J. Clin. Anes.* **1995**, *7*, 558–563. (c) Scholz, J.; Steinfath, M. Ist Remifentanyl ein Ideales Opioid für das anästhesiologische Management im 21. Jahrhundert? *Anästhesiol Intensivmed. Notfallmed. Schmerzther.* **1996**, *31*, 592–607.
- (17) James, M. K.; Vuong, A.; Grizzle, M. K.; Shuster, S. V.; Shaffer, J. E.; Hemodynamic Effects of GI 87084B, An Ultra-short Acting  $\mu$ -opioid Analgesic in Anesthetized Dogs. *J. Pharmacol. Exp. Ther.* **1992**, *263*, 84–91.
- (18) Zhu, J.; Xue, J.-C.; Law, P.-Y.; Claude, P. A.; Luo, L.-Y.; Yin, J.-L.; Chen, C.-G.; Liu-Chen, L.-Y. The Region in the  $\mu$  Opioid Receptor Conferring Selectivity for Sufentanil over the  $\delta$  Receptor is Different from that over the  $\kappa$  Receptor. *FEBS Lett.* **1996**, *384*, 198–202.
- (19) Heerding, J.; Raynor, K.; Kong, H.; Yu, L.; Reisine, T. Mutagenesis Reveals that Agonists and Peptide Antagonists Bind in Fundamentally Distinct Manners to the Rat Mu Receptor than do Nonpeptide Antagonists. *Reg. Pept.* **1994**, *54*, 119–120.
- (20) (a) Mansour, A.; Taylor, L. P.; Fine, J. L.; Thompson, R. C.; Hoversten, M. T.; Mosberg, H. I.; Watson, S. J.; Akil, H. Key Residues Defining the  $\mu$ -opioid Receptor Binding Pocket: A Site-directed Mutagenesis Study. *J. Neurochem.* **1997**, *68*, 344–353. (b) Bot, G.; Blake, A. D.; Li, S.-X.; Resine, T. Fentanyl and its Analogues Desensitize the Cloned Mu Opioid Receptor. *J. Pharmacol. Exp. Ther.* **1998**, *285*, 1207–1218.
- (21) Lu, Y.-F.; Xu, H.; Liu-Chen, L.-Y.; Chen, C.-G.; Partilla, J. S.; Brine, G. A.; Carroll, F. I.; Rice, K. C.; Lai, J.; Porreca, F.; Sadee, W.; Rothman, R. B. Opioid Peptide Receptor Studies. 7. The Methylfentanyl Congener RTI-4614-4 and its Four Enantiomers Bind to Different Domains of the rat  $\mu$  Opioid Receptor. *Synapse* **1998**, *28*, 117–124.
- (22) Pogozheva, I. D.; Lomize, A. L.; Mosberg, H. I. Opioid Receptor Three-dimensional Structures from Distance Geometry Calculations with Hydrogen Bonding Constraints. *Biophys. J.* **1998**, *75*, 612–634.
- (23) Tollenaere, J. P.; Moereels, H.; van Loon, M. On Conformation Analysis, Molecular Graphics, Fentanyl and its Derivatives. *Prog. Drug Res.* **1986**, *30*, 91–126.
- (24) Brandt, W.; Barth, A.; Hölthje, H.-D. A New Consistent Model Explaining Structure (Conformation)-activity Relationships of Opiates with  $\mu$ -selectivity. *Drug Des. Discov.* **1993**, *10*, 257–283.
- (25) Martins, J.; Andrews, P. Conformation-activity Relationships of Opiate Analgesics. *J. Comput.-Aided Mol. Des.* **1987**, *1*, 53–72.
- (26) (a) Cometta-Morini, C.; Loew, G. H. Development of a Conformational Search Strategy for Flexible Ligands: A Study of the Potent  $\mu$ -selective Opioid Analgesic Fentanyl. *J. Comput.-Aided Mol. Des.* **1991**, *5*, 335–356 and references therein. (b) Cometta-Morini, C.; Maguire, P. A.; Loew, G. H. Molecular Determinants of  $\mu$  Receptor Recognition for the Fentanyl Class of Compounds. *Mol. Pharmacol.* **1992**, *41*, 185–196.
- (27) Rong, S.-B.; Zhu, Y.-C.; Jiang, H.-L.; Wang, Q.-M.; Zhao, S.-R.; Chen, K.-X.; Ji, R.-Y. Interaction Models of 3-Methylfentanyl Derivatives with  $\mu$  Opioid Receptors. *Acta Pharmacol. Sin.* **1997**, *18*, 128–132.
- (28) Baldwin, J. M.; Schertler, G. F. X.; Unger, V. M. An Alpha-carbon Template for the Transmembrane Helices in the Rhodopsin Family of G-protein-coupled Receptors. *J. Mol. Biol.* **1997**, *272*, 144–164.
- (29) (a) Paterlini, G.; Portoghese, P. S.; Ferguson, D. M. Molecular Simulation of Dynorphin A(1–10) Binding to Extracellular Loop 2 of the  $\kappa$ -opioid Receptor. A Model for Receptor Activation. *J. Med. Chem.* **1997**, *40*, 3254–3262. (b) Subramanian, G.; Paterlini, M. G.; Larson, D. L.; Portoghese, P. S.; Ferguson, D. M. Conformational Analysis and Automated Receptor Docking of Selective Arylacetamide-Based  $\kappa$ -opioid Agonists. *J. Med. Chem.* **1998**, *41*, 4777–4789.
- (30) Unger, V. M.; Hargrave, P. A.; Baldwin, J. M.; Schertler, G. F. X. Arrangement of Rhodopsin Transmembrane Alpha Helices Obtained by Electron Cryo-microscopy. *Nature* **1997**, *389*, 203–206.
- (31) Metzger, T. G.; Paterlini, M. G.; Portoghese, P. S.; Ferguson, D. M. Application of the Message-Address Concept of the Docking of Naltrexone and Selective Naltrexone-Derived Opioid Antagonists into Opioid Receptor Models. *Neurochem. Res.* **1996**, *21*, 1287–1294.
- (32) Dunbrack, R. L., Jr.; Karplus, M. Backbone-dependent Rotamer Library for Proteins. Application to Side-chain Prediction. *J. Mol. Biol.* **1993**, *230*, 543–574.
- (33) Xu, W.; Ozdener, F.; Li, J.-G.; Chen, C.; de Riel, J. K.; Weinstein, H.; Liu-Chen, L.-Y. Functional Role of the Spatial Proximity of Asp114(2.50) in TMH 2 and Asn332(7.49) in TMH 7 of the  $\mu$  Opioid Receptor. *FEBS Lett.* **1999**, *447*, 318–324.
- (34) Zhou, W.; Flanagan, C.; Ballesteros, J. A.; Konvicka, K.; Davidson, J. A.; Weinstein, H.; Millar, R. P.; Sealfon, S. C. A Reciprocal Mutation Supports Helix 2 and Helix 7 Proximity in the Gonadotropin-releasing Hormone Receptor. *Mol. Pharmacol.* **1994**, *45*, 165–170.
- (35) Javitch, J. A.; Fu, D.; Chen, J. Residues in the Fifth Membrane-spanning Segment of the Dopamine D2 Receptor Exposed in the Binding-site Crevise. *Biochemistry* **1995**, *34*, 16433–16439.
- (36) Perlman, J. H.; Colson, A. O.; Wang, W.; Bence, K.; Osman, R.; Gershengorn, M. C. Interaction Between Conserved Residues in Transmembrane Helices 1, 2, and 7 of the Thyrotropin-releasing Hormone Receptor. *J. Biol. Chem.* **1997**, *272*, 11937–11942.
- (37) Thirstrup, K.; Elling, C. E.; Hjorth, S. A.; Schwartz, T. W. Construction of a High Affinity Zinc Switch in the  $\kappa$ -opioid Receptor. *J. Biol. Chem.* **1996**, *271*, 7875–7878.
- (38) Laskowski, R. A.; MacArthur, M. W.; Moss, D. S.; Thornton, J. M. PROCHECK: A Program to Check the Stereochemical Quality of Protein Structures. *J. Appl. Crystallogr.* **1993**, *26*, 283–291.
- (39) Peeters, O. M.; Blaton, N. M.; De Ranter, C. J.; van Herk, A. M.; Goubitz, K. Crystal and Molecular Structure of N-[1-(2-phenylethyl)-4-piperidinium]-N-phenylpropanamide (fentanyl) citrate-toluene Solvate. *J. Cryst. Mol. Struct.* **1979**, *9*, 153–161.
- (40) Koch, M. H. J.; De Ranter, C. J.; Rolies, M.; Dideberg, O. *Acta Crystallogr.* **1976**, *B32*, 2529.
- (41) Flippin-Anderson, J. L.; George, C.; Bertha, C. M.; Rice, K. C. X-ray Crystal Structures of Potent Opioid Receptor Ligands: Etonitazene, *cis*-(+)-3-Methylfentanyl, Etorphine, Diprenorphine, and Buprenorphine. *Heterocycles* **1994**, *39*, 751–766.
- (42) Brine, G. A.; Stark, P. A.; Liu, Y.; Carroll, F. I.; Singh, P.; Xu, H.; Rothman, R. B. Enantiomers of Diastereomeric *cis*-N-[1-(2-Hydroxy-2-phenylethyl)-3-methyl-4-piperidyl]-N-phenylpropanamides: Synthesis, X-ray Analysis, and Biological Activities. *J. Med. Chem.* **1995**, *38*, 1547–1557.
- (43) Frisch, M. J.; Trucks, G. W.; Schlegel, H. B.; Gill, P. M. W.; Johnson, B. G.; Robb, M. A.; Cheeseman, J. R.; Keith, T.; Petersson, G. A.; Montgomery, J. A.; Raghavachari, K.; Al-Laham, M. A.; Zakrzewski, V. G.; Ortiz, J. V.; Foresman, J. B.; Cioslowski, J.; Stefanov, B. B.; Nanayakkara, A.; Challacombe, M.; Peng, C. Y.; Ayala, P. Y.; Chen, W.; Wong, M. W.; Andres,



- J. L.; Replogle, E. S.; Gomperts, R.; Martin, R. L.; Fox, D. J.; Binkley, J. S.; Defrees, D. J.; Baker, J.; Stewart, J. J. P.; Head-Gordon, M.; Gonzalez, C.; Pople, J. A. *Gaussian94*, revision E2; Gaussian Inc.: Pittsburgh, PA, 1995.
- (44) Cieplak, P.; Cornell, W. D.; Bayly, C.; Kollman, P. A. Application of the Multimolecule and Multiconformational RESP Methodology to Biopolymers: Charge Derivation for DNA, RNA, and Proteins. *J. Comput. Chem.* **1995**, *16*, 1357–1377.
- (45) Cornell, W. D.; Cieplak, P.; Bayly, C. I.; Gould, I. R.; Merz, K. M., Jr.; Ferguson, D. M.; Spellmeyer, D. C.; Fox, T.; Caldwell, J. W.; Kollman, P. A. A Second Generation Force Field for the Simulation of Proteins, Nucleic Acids, and Organic Molecules. *J. Am. Chem. Soc.* **1995**, *117*, 5179–5197.
- (46) (a) Pearlman, D. A.; Case, D. A.; Caldwell, J. W.; Ross, W. S.; Cheatham, T. E., III; Debolt, S.; Ferguson, D. M.; Seibel, G. L.; Kollman, P. A. AMBER, a Package of Computer Programs for Applying Molecular Mechanics, Normal-mode Analysis, Molecular Dynamics, and Free Energy Calculations to Simulate the Structural and Energetic Properties of Molecules. *Comput. Phys. Commun.* **1995**, *91*, 1–41. (b) Pearlman, D. A.; Case, D. A.; Caldwell, J. W.; Ross, W. S.; Cheatham, T. E., III; Ferguson, D. M.; Seibel, G. L.; Singh, U. C.; Weiner, P. K.; Kollman, P. A. *AMBER*, version 4.1; Department of Pharmaceutical Chemistry, University of California: San Francisco, CA, 1995.
- (47) Fox, T.; Scanlan, T. S.; Kollman, P. A. Ligand Binding in the Catalytic Antibody 17E8. A Free Energy Perturbation Calculation Study. *J. Am. Chem. Soc.* **1997**, *119*, 11571–11577.
- (48) Jorgenson, W. L.; Chandrasekhar, J.; Madhura, J. D.; Impey, R. W.; Klein, M. L. Comparison of Simple Potential Functions for Simulating Liquid Water. *J. Chem. Phys.* **1983**, *79*, 926–935.
- (49) Berendsen, H. J. C.; Postma, J. P. M.; van Gunsteren, W. F.; DiNola, A.; Haak, J. R. Molecular Dynamics with Coupling to an External Bath. *J. Chem. Phys.* **1984**, *81*, 3684–3690.
- (50) (a) Meng, E. C.; Shoichet, B. K.; Kuntz, I. D. Automated Docking with Grid-based Energy Evaluation. *J. Comput. Chem.* **1992**, *13*, 505–524. (b) Meng, E. C.; Gschwend, D. A.; Blaney, J. M.; Kuntz, I. D. Orientational Sampling and Rigid-body Minimization in Molecular Docking. *Proteins: Struct. Funct. Genet.* **1993**, *17*, 266–278. (c) Connolly, M.; Gschwend, D. A.; Good, A. C.; Oshiro, C.; Kuntz, I. D. *DOCK*, version 3.5; Department of Pharmaceutical Chemistry, University of California: San Francisco, CA, 1995.
- (51) (a) Connolly, M. L. Solvent-accessible Surfaces of Proteins and Nucleic Acids. *Science* **1983**, *221*, 709–713. (b) Connolly, M. L. Analytical Molecular Surface Calculation. *J. Appl. Crystallogr.* **1983**, *16*, 548–558.
- (52) (a) Surratt, C. K.; Johnson, P. S.; Moriwaki, A.; Seidleck, B. K.; Blaschak, C. J.; Wang, J. B.; Uhl, G. R.  $\mu$  Opiate Receptor. *J. Biol. Chem.* **1994**, *269*, 20548–20553. (b) Befort, K.; Tabbara, L.; Bausch, S.; Chavkin, C.; Evans, C.; Kieffer, B. The Conserved Aspartate Residue in the Third Putative Transmembrane Domain of the  $\mu$ -opioid Receptor is not the Anionic Counterpart for Cationic Opiate Binding but is a Constituent of the Receptor Binding Site. *Mol. Pharmacol.* **1996**, *49*, 216–223.
- (53) (a) Castiglione-Morelli, M. A.; Lelj, F.; Pastore, A.; Salvadori, S.; Tancredi, T.; Tomatis, R.; Trivellone, E. A 500-MHz Proton Nuclear Magnetic Resonance Study of  $\mu$  Opioid Peptides in a Simulated Receptor Environment. *J. Med. Chem.* **1987**, *30*, 2067–2073. (b) Brine, G. A.; Boldt, K. G.; Huang, P.-T.; Sawyer, D. K.; Carroll, F. I. Carbon-13 Nuclear Magnetic Resonance Spectra of Fentanyl Analogues. *J. Heterocycl. Chem.* **1989**, *26*, 677–686.
- (54) Attempts to identify a probable docking arrangement for the highly sampled  $[g^+, g^+, g^-]$  and  $[g^+, g^+, g^+]$  solution conformations for **4** and **6** resulted in initial docking arrangements where the ligands occupied the larger pocket between TM-III and -V–VII helices and are not consistent with experimental point mutation results and the binding modes of other members in this series.
- (55) Hjorth, S. A.; Thirstrup, K.; Grandy, D. K.; Schwartz, T. W. Analysis of Selective Binding Epitopes for the  $\kappa$ -opioid Receptor Antagonist Nor-binaltorphimine. *Mol. Pharmacol.* **1995**, *47*, 1089–1094.
- (56) (a) Jones, R. M.; Hjorth, S. A.; Schwartz, T. W.; Portoghese, P. S. Mutational Evidence for a Common  $\kappa$  Antagonist Binding Pocket in the Wild-type  $\kappa$  and Mutant  $\mu$ [K303E] Opioid Receptors. *J. Med. Chem.* **1998**, *41*, 4911–4914. (b) Stevens, W. C., Jr.; Jones, R. M.; Subramanian, G.; Metzger, T. G.; Ferguson, D. M.; Portoghese, P. S. Potent and Selective Indolomorphinan Antagonists of the  $\kappa$ -Opioid Receptor. *J. Med. Chem.*, manuscript in preparation.
- (57) Valiquette, M.; Vu, H. K.; Yue, S. Y.; Wahlestedt, C.; Walker, P. Involvement of Trp-284, Val-296, and Val-297 of the Human  $\delta$ -opioid Receptor Binding of  $\delta$ -selective Ligands. *J. Biol. Chem.* **1996**, *271*, 18789–18796.
- (58) Kong, H.; Raynor, K.; Reisine, T. Amino Acids in the Cloned Mouse Kappa Receptor That are Necessary for High Affinity Agonist Binding but not Antagonist Binding. *Reg. Pept.* **1994**, *54*, 155–156.
- (59) Spivak, C. E.; Beglan, C. L.; Seidleck, B. K.; Hirshbein, L. D.; Blaschak, C. J.; Uhl, G. R.; Surratt, C. K. Naloxone Activation of  $\mu$ -opioid Receptors Mutated at a Histidine Residue Lining the Opioid Binding Cavity. *Mol. Pharmacol.* **1997**, *52*, 983–992.
- (60) Tang, Y.; Chen, K. X.; Jiang, H. L.; Wang, Z. X.; Ji, R. Y.; Chi, Z. Q. Molecular Modeling of  $\mu$  Opioid Receptor and its Interaction with Ohmefentanyl. *Acta Pharmacol. Sin.* **1996**, *17*, 156–160.
- (61) Xu, H.; Lu, Y.-F.; Partilla, J. S.; Zheng, Q.-X.; Wang, J.-B.; Brine, G. A.; Carroll, I.; Rice, K. C.; Chen, K.-X.; Chi, Z.-Q.; Rothman, R. B. Opioid Peptide Receptor Studies, 11: Involvement of Tyr148, Trp318 and His319 of the Rat  $\mu$ -Opioid Receptor in Binding of  $\mu$ -Selective Ligands. *Synapse* **1999**, *32*, 23–28.
- (62) Riley, T. N.; Hale, D. B.; Wilson, M. C. 4-Anilidopiperidine Analgesics I: Synthesis and Analgesic Activity of Certain Ring-methylated 1-substituted 4-propananilidopiperidines. *J. Pharm. Sci.* **1973**, *62*, 983–986.
- (63) Casy, A. F.; Ogunbamila, F. O. 3-Allyl and 3-Propyl Analogues of Fentanyl. *Eur. J. Med. Chem. – Chim. Ther.* **1983**, *18*, 56–60.
- (64) Maryanoff, B. E.; McComsey, D. F.; Taylor, R. J., Jr.; Gardocki, J. F. Synthesis and Stereochemistry of 7-Phenyl-2-propionanilidobenzo[a]quinolizidine Derivatives. Structural Probes for Fentanyl Analgesics. *J. Med. Chem.* **1981**, *24*, 79–88.
- (65) Bagley, J. R.; Thomas, S. A.; Rudo, F. G.; Spencer, H. K.; Doorley, B. M.; Ossipov, M. H.; Jerussi, T. P.; Benvenga, M. J.; Spaulding, T. New 1-(Heterocyclylalkyl)-4-propionanilido-4-piperidinyl Methyl Ester and Methylene Methyl Ether Analgesics. *J. Med. Chem.* **1991**, *34*, 827–841.
- (66) (a) Janssen, P. A. J.; van der Eycken, C. A. M. The Chemical Anatomy of Potent Morphine like Analgesics. In *Drugs Affecting the CNS*; Burger, A., Ed.; Dekker: New York, 1968; Vol. 2, pp 25–60. (b) Klein, W.; Back, W.; Mutschler, E. Über die Synthese und Pharmakologische Wirkung Cyclicher Analoga des Fentanyls. *Arch. Pharm.* **1975**, *308*, 910–914. (c) Berger, J. G.; Davidson, F.; Langford, G. E. Synthesis of Some Conformationally Restricted Analogues of Fentanyl. *J. Med. Chem.* **1977**, *20*, 600–602. (d) Borne, R. F.; Fifer, E. K.; Waters, I. W. Conformationally Restrained Fentanyl Analogues. 2. Synthesis and Analgesic Evaluation of Perhydro-1,6-naphthyridin-2-ones. *J. Med. Chem.* **1984**, *27*, 1271–1275.
- (67) (a) Clark, R. L.; Pessolano, A. A.; Weijlard, J.; Pfister, K. N-substituted Epoxymorphinans. *J. Am. Chem. Soc.* **1953**, *75*, 4963–4967. (b) Winter, C. A.; Orashevats, P. D.; Lehman, E. G. Analgesic Activity and Morphine Antagonism of Compounds Related to Nalorphine. *Arch. Int. Pharmacodyn.* **1957**, *CX*, 186–202.
- (68) Kong, H.; Raynor, K.; Yasuda, K.; Moe, S. T.; Portoghese, P. S.; Bell, G. I.; Reisine, T. A Single Residue, Aspartic Acid 95, in the  $\delta$  Opioid Receptor Specifies Selective High Affinity Agonist Binding. *J. Biol. Chem.* **1993**, *268*, 23055–23058.
- (69) Shieh, T.; Han, M.; Sakmar, T. P.; Smith, S. O. The Steric Trigger in Rhodopsin Activation. *J. Mol. Biol.* **1997**, *269*, 373–384.
- (70) (a) Bagley, J. R.; Wynn, R. L.; Rudo, F. G.; Doorley, B. M.; Spencer, H. K.; Spaulding, T. New 4-(Heteroanilido)piperidines, Structurally Related to the Pure Opioid Agonist Fentanyl, with Agonist and/or Antagonist Properties. *J. Med. Chem.* **1989**, *32*, 663–671. (b) Kudzma, L. V.; Severnak, S. A.; Benvenga, M. J.; Ezell, E. F.; Ossipov, M. H.; Knight, V. V.; Rudo, F. G.; Spencer, H. K.; Spaulding, T. C. 4-Phenyl- and 4-Heteroaryl-4-anilidopiperidines. A Novel Class of Analgesic and Anesthetic Agents. *J. Med. Chem.* **1989**, *32*, 2534–2542. (c) France, C. P.; Ahn, S. C.; Brockunier, L. L.; Bagley, J. R.; Brandt, M. R.; Winsauer, P. J.; Moerschbaecher, J. M. Behavioral Effects and Binding Affinities of the Fentanyl Derivative OHM3507. *Pharmacol. Biochem. Behav.* **1998**, *59*, 295–303.